Contemporary Engineering Sciences, Vol. 9, 2016, no. 11, 513 - 530
HIKARI Ltd, www.m-hikari.com
http://dx.doi.org/10.12988/ces.2016.6320

Fatigue Strength Analysis of Welded Joints Using an Experimental Approach Based on Static Characterization Tests

Hamza Khatib

Laboratory of Physics, Condensed Matter and Renewable Energy
University of Science and Technology, Mohammedia, Morocco

Khalifa Mansouri

Laboratory of Signals, Distributed Systems and Artificial Intelligence, ENSET Mohammedia, Morocco

Bachir Salhi

Mechanics Research Group, ENSET, Rabat, Morocco

Abderrahmane Yeznasni

Laboratory of Physics, Condensed Matter and Renewable Energy
University of Science and Technology, Mohammedia, Morocco

Abstract

This research proposes an approach to estimate the fatigue life of the weld bead. The results obtained using this approach will be used to analyze the notch effects on the fatigue life of welded joints. Two joint configurations are analyzed at the end of this paper.

The paper include two main parts, the first section will focus on calculating the fatigue curve (σ-N) of the welded joint. These calculations are based on the local deformations approach (ε-N) that requires fatigue parameters related to material strength. Determination of these parameters will be provided through a set of correla-

tion formulas and static characterization tests. At the end of this part, the calculated fatigue curve (σ-N), will be compared to other curves of three different materials in order to evaluate the accuracy of results.
The second part of this work presents an analysis of the notch effect on the fatigue strength. Two welded joint configurations are subjected to these analyses, the calculations aims to determine the fatigue curve for each joint that will be compared to the values recommended by standards of the steel structures.

Keywords: Fatigue strength, welded joint, notch effect, volumetric approach

1-Introduction

Steel structures involve various joining techniques including welding, which is used for many reasons. This is related to the required time for the process execution and also related to the affordable cost with good reliability. These structures are subjected during their life cycle, to variable load components due to the external environment (such as wave and wind impact). Introducing the welded joints in structures subjected to fatigue loads creates a challenge to insure the structural strength. This situation needs a better knowledge of fatigue behavior of the welded joints. Estimating this behavior using the fatigue tests is the most reliable method, however, it requires a significant investment in time and resources, which make this solution not affordable for a large majority of industrial actors in steel construction.
To conclude the fatigue parameters of welded joints, our approach relies on using results of shorter and less expensive tests (tensile tests and hardness tests), these results provide a good understanding of fatigue behavior through equations developed for this purpose. The development of these equations is based on a many experimental results stored into specialized databases [22], the analysis of these results shows a strong correlation between the static mechanical properties (HB, E, Re, Rm ..) and fatigue mechanical properties (b, c, σ'_f, ε'_f, σ_D ...).

2 Fatigue strength of welded joint

Our goal during this section is to estimate the fatigue curve (σ-N) of the weld joint. To achieve this purpose, the first step is devoted to experimental work in order to measure the mechanical behavior of the base and the filler metal (Figure-1). The tensile tests on the base metal and on the welded joint will enable us to identify the mechanical parameters (Rm, Re, A%) and their fluctuation after welding. The second step aims to estimate the true tensile curve (σ-ε) in cyclic regime, this curve is obtained according to the Ramberg-Osgood model which requires the identification of two parameters (n') and (K'). The third calculating step is dedicated to determine the fatigue strength based on the local deformations approach, this approach will allow us to deduce the fatigue resistance through the Manson-Coffin expression, identification of the parameters (b, c, ε'_f, σ'_f) is ensured by using results of the experimental tests and correlation expressions.

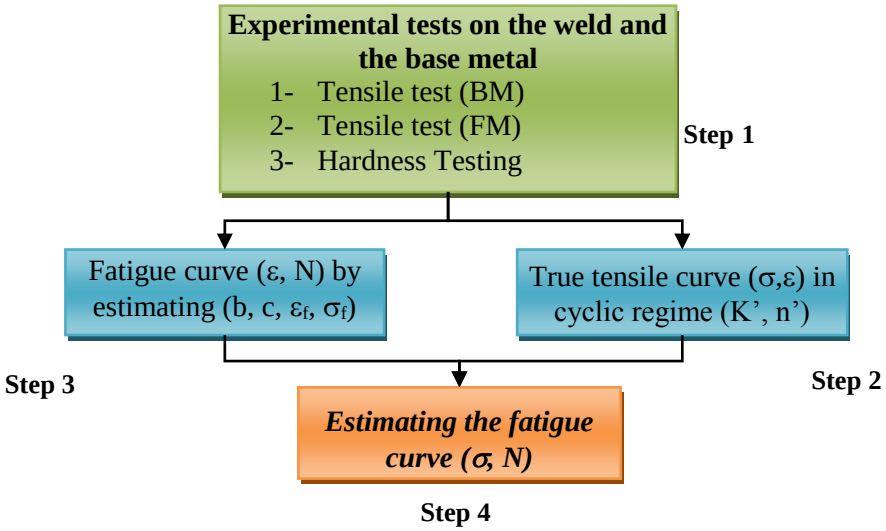

Figure 1 : Steps for estimating the fatigue curve

The final step aims to determine the fatigue curve (σ-N) by using results of the local deformation approach (ε-N) and the true tensile curve (σ-ε).

2-1 Characterization tests of the base metal and welded joint

The studied weld bead is carried out by using basic electrode with low hydrogen content. This electrode ensures a good homogeneity of the weld and limits the cracks initiation [8] [3]. The electrodes used in our case (E7018), are applied for joints subjected to radiographic or ultrasonic inspection. The welding procedure is initiated by preparing the tow surfaces to be joined and by drying the electrodes at high temperature to ensure a stable arc during welding process without interruptions.

Base metal characterization - tensile test

The base metal used is S235 steel (E-24), chemical composition (Table-1) shows an alloy which belongs to the mild steels with low carbon content. This composition justifies its good weldability which is highly recommended in steel constructions.

C	Mn	P	Si	N
0,17% Max	1,4% Max	0,035% Max	0,035% Max	0,012% Max

Table 1- Chemical composition of the base metal

Table-2 includes the mechanical properties of base metal obtained from tensile tests, the results show that the A36 and A284 steels (ASTM) are closest to the S235 steel in terms of mechanical behavior.

Yield Stress (Re)	Ultimate strength (Rm)	Young's Modulus (E)
321 MPa	**405 MPa**	**210 GPa**

Table 2-Results of the tensile tests obtained on the base metal

Characterization of the weld joint - Tensile tests

The composition and the mechanical behavior of the filler metal provided by the manufacturer are illustrated in the following tables.

C	Mn	S
0,08%	1,2%	0,5%

Table 3- chemical composition of the filler metal

Re (MPa)	Rm (MPa)
520	590

Table 4- Mechanical properties of the filler metal

The homogeneity between the filler and base metal properties is the main difficulty in order to estimate the mechanical behavior of the weld joint. A macro mechanical characterization of the tensile strength will be operated on middle welded bead.

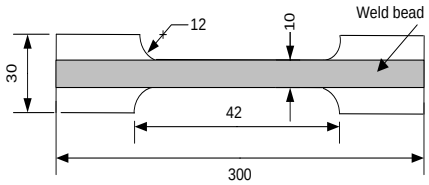

(a)

(b)

Figure 2- Welded specimen used during tensile test

Yield Stress (Re)	Ultimate strength (Rm)	E	Rm/Re	$\Delta l/l_0$
361 MPa	430 MPa	204,6 GPa	1,19	25,5%

Table 5- Mechanical behavior of the welded specimen

The obtained results shows that filler metal provides an improvement to mechanical strength with maintaining a good ductility; the results confirm an elongation of 25.5% and 30% of reduction of the cross section area.

Local characterization of the weld bead- Hardness Measurement

Local characterization of the welded joint by hardness measurement will illustrate the effects of welding on the static and cyclic mechanical properties. Through

several research, it is recognized that the results of tensile tests have a strong correlation with the hardness results, an example of expressions relating the static strength (Rm) and the hardness (HB) is given by equations 1 and 2 [4].

$$Rm = 3{,}45x(HB) \quad (1)$$

$$Rm = 0{,}0012(HB)^2 + 3{,}3(HB) \quad (2)$$

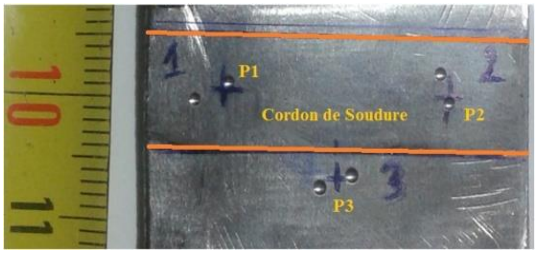

Figure 3 : Specimen used during hardness measurement

In order to visualize the local mechanical behavior of the weld bead, local mechanical strength (Rm) was calculated from the hardness measurements. The values of (Rm) are obtained from equation 1 which will be adjusted to our material case. From the measurements obtained on the base metal, the ratio (Rm/HB) will be taken to a value of 3.2. The following table summarizes the hardness obtained at different measurement points.

Point	Distance from weld (mm)	Hardness (HB1)	Hardness (HB2)	Average hardness (HBm)	Tensile strength (MPa)
P1	0	195	173	**184**	**588,8**
P2	0	194	189	**191,5**	**612,8**
P3	7	125	135	**130**	**416**
P4	15	131	129	**130**	**416**

Table 6 : Results of hardness measurement

The results show the variation of the mechanical behavior by moving away from the centerline of the weld bead. The point maximizing the hardness curve gives 600 MPa as an average of mechanical strength which approach the supplier's data (Table 4).

2-2 Tensile strength (σ, ε) of the welded joint

Ramberg-Osgood Model

Steel mechanical behavior changes by applying a cyclic load. This phenomenon analyzed by Bauschinger [21] shows that, after several tensile cycles, the variation

of the mechanical strength (Rm) can reach high values. The modification may be in the form of a hardening which improves the mechanical properties or in the form of softening. These changes cause also a variation of the Ramberg-Osgood parameters [19] that will be denoted by (E', n', K') in the cyclic case; and which are a function of number of cycles applied n'(N), K'(N), E'(N). An experimental observation shows that these properties are stabilized after several cycles (the values are generally given for the half life of the specimen).

$$\varepsilon = \frac{\sigma}{E} + \left(\frac{\sigma}{K'}\right)^{\frac{1}{n'}} \tag{3}$$

The estimation of the cyclical parameters may be conducted using the models developed and based on experimental results [22]. The experimental work of A. Fatemi [20] [12] provides a set of relationships based on these results.

- Strain hardening coefficient from the Brinell hardness (HB=140) :

$$K' = 9{,}8x10^{-3}(HB)^2 - 1{,}26(HB) + 705 = \mathbf{720{,}68\ MPa} \tag{4}$$

- Hardening exponent based on mechanical strength

$$n' = -0{,}37 \ln\left(\frac{0{,}75R_e + 82}{1{,}16R_m + 593}\right) = 0{,}188 \tag{5}$$

Strain hardening coefficient K’	Hardening exponent n’
721 MPa	0,188

2-3 Fatigue Curve (ε-N)

The analysis of the fatigue strength using local deformation curve (ε-N) is an approach which is increasingly used to estimate the fatigue life duration in low cycle fatigue (LCF); especially in the case of the local stress concentration [10]. The calculation models includes, in addition of the elastic deformation which govern the high-cycle fatigue (HCF) regime, a plastic deformation and its effect on the fatigue life. Generally, the effect of plastic deformation can be represented by a linear logarithmic relation, as well as for the effect of the elastic component.

$$\frac{\Delta\varepsilon}{2} = \varepsilon_a = \frac{\Delta\varepsilon_e}{2} + \frac{\Delta\varepsilon_p}{2} = \underbrace{\frac{\sigma'_f}{E}(N)^b}_{Elastic} + \underbrace{\varepsilon'_f(N)^c}_{Plastic} \tag{6}$$

Estimation of the fatigue parameters under controlled strain.

The estimation of the parameters (b, ε’f, c, σ’f) is performed by using the following expressions [20] [12]:

$$\varepsilon'_f = \frac{0{,}004*(HB)^2 + 1{,}15(HB)}{E(10^{5{,}755-0{,}0071HB})^{-0{,}56}} = 0{,}542 \tag{7}$$

$$\sigma_f^{'} = K^{'}\left(\varepsilon_f^{'}\right)^{\frac{b}{c}} = 788{,}263\text{MPa} \quad (8)$$

$$b = \frac{-n'}{1+5n'} = -9{,}47\ 10^{-2} \quad (9)$$

$$c = \frac{-1}{1+5n'} = -0{,}526 \quad (10)$$

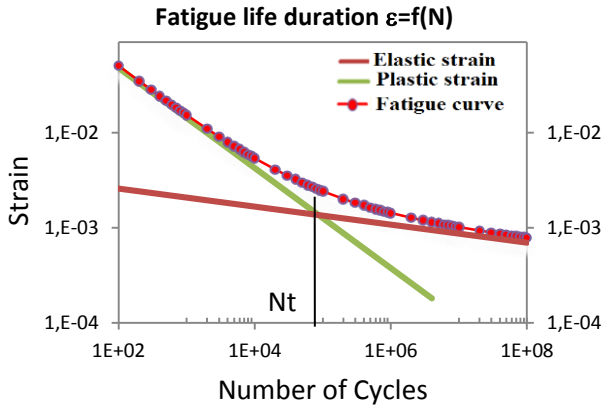

Figure 4 : Fatigue life duration as a function of the local deformation

2-4 Fatigue curve (σ-N)

Fatigue curves (σ-N) are more used in high cycle fatigue regime (HCF) which is characterized by low strain. This regime is characterized by crack initiation caused by dislocations that propagate to the workpiece surface, this phenomenon gives rise to many slip bands which accumulate and become more evident [9]. The estimation of the endurance limit (σ_D) is an experimental problem. Moore's book [14] contains a large number of experimental results; analyzing the variation of the endurance limit (σ_D) with respect to the mechanical strength (Rm) for different steel grades shows that the (σ_D) is strongly correlated to the mechanical strength (Rm). Experimental work of Gaugh [13] conducted on specimens with mechanical strength (Rm) ranging from 310 MPa to 2000MPa, specifies that the endurance limit (σ_D) can be limited in the interval [0,46xRm; 0,54xRm].

$$N = N_f\left(\frac{\sigma_f}{\sigma_a}\right)^{2k-1} \quad (11)$$

k=-1/B

The estimation of the fatigue curve will be based on the values obtained from fatigue curve (ε-N) and also based on the Haibach Model which take into account the transition around (σ_D). It clearly appears that the Basquin line approaches the fatigue curve more precisely during (HCF) regime; the intersection between the two curves are observed at $N=8.10^6$.

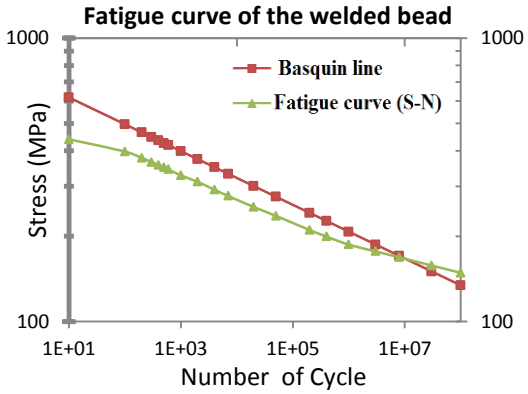

Figure 5 : Fatigue curve calculated and compared to the Basquin line

2-5 Comparative analysis of the obtained results

The fatigue results obtained on three different materials were used during this analysis to evaluate the accuracy of our calculation.

[7]: A36 Steel; [2]: MS4361 Steel; [3]: 0030 stainless steel

Steel	Re	Rm	E	n'	K'	c	ε_f	B	σ_f
S235	**361**	**430**	**204,6**	**0,188**	**721**	**-0,526**	**0,542**	**-0,094**	**788**
A36 [7]	408	580	189	0,197	1235	-0,567	0,602	-0,09	1028
MS4361 [2]	414	625	198,2	0,169	1010	-0,463	0,207	-0,078	775
0030 [3]	303	496	207	0,169	887	-0,518	0,212	-0,091	704

Table 7 : Fatigue properties of the material used and the other three materials

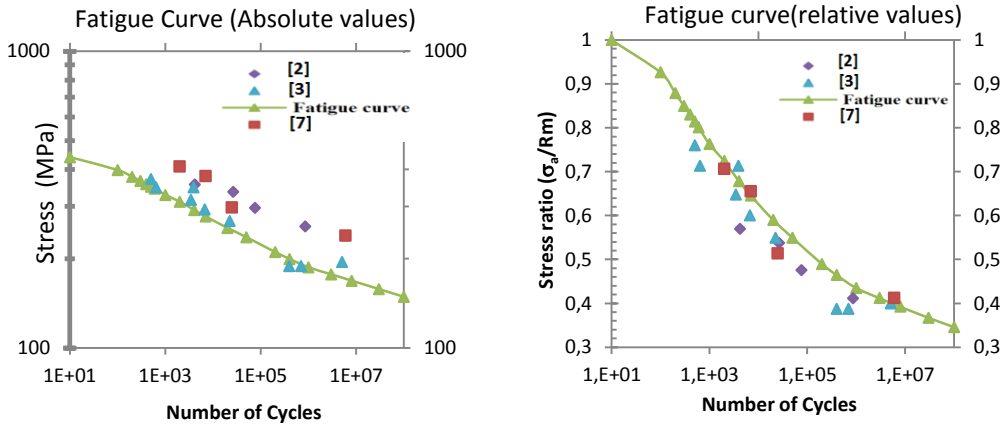

(a) (b)

Figure 6 : fatigue curves compared to the results obtained on other materials
(a) : Representation in absolute values (b) : Representation in relative values

A first representation of the obtained results shows a deviation from the fatigue results obtained on materials [6] and [2]. This difference is justified by strength of these two materials which have higher mechanical features. It is noted however that the fatigue performance of the material [2] provides a good fit with our results. This match is explained by the reconciliation between the mechanical properties of these two materials, these results validate the benefit and the accuracy of our results already achieved.
A second analysis show the evolution of the stress ratio (σ_a/Rm) related to the number of cycles (N) which will reduce the effect of the mechanical strength (Rm) of the both materials [6], [2]. The results show that the gap between the three different materials is very limited mainly between A36 steel [6] and our material. The results above show an acceptable difference with a slight increase in number of cycles obtained.

3- Fatigue strength of weld bead in the case of stress concentration

This second part presents an analysis of the notch effect on the fatigue strength of the welded joints. The fatigue life reduction introduced by the notch effect will be measured through the fatigue reduction factor (kf). Two types of weld joint are analyzed (Butt joint and T joint). The choice of these two first configurations will allow us to clearly evaluate the used calculation models. Results will be compared with the recommended standard values and the experimental results of some other researches. For each type of weld joint, a first analysis of the stress field will be established based on the finite elements and using the mechanical properties of the material already obtained. The analysis of the stress field in the vicinity of the notch will allow to deduce subsequently the fatigue reduction factor (Kf) calculated by different approaches and for different loads applied. The fatigue curve of each joint will be evaluated by using the (Kf) factor and the reference fatigue curve (fatigue curve of the weld bead).

3-1 Butt welded joint, effect of the toe radius

In the case of butt welded joints, the effect of the radius in the butt joint is important especially for high reliability structures that are loaded cyclically. The aim of this part is to deduce the effect of this type of notch on the (Kf) factor with taking into account the nonlinear behavior of the used material.

Geometrical parameters and the linear modeling results

The weld bead is achieved by rounding the weld root with an abrasive cylinder (R=1.5mm). The plate used to produce the weld has a thickness of 3mm and the weld bead has a height of 2.1mm from the surface of the plate. Modeling the weld bead with a 1.5mm radius and under tensile load of 1 MPa gives an elastic stress concentration factor (Kt=1.7), the stress concentration area is located on the weld toe which is the most exposed area to the crack initiation.

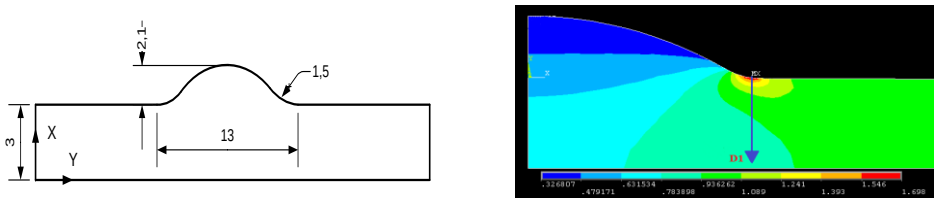

(a) (b)

Figure 7 : Numerical modeling of the stress field
(a) : geometrical parameters of the weld ; (b) : The stress field and analysis direction

The elasto-plastic analysis results

Modeling the stress field is performed on ANSYS using a 2D model, the mesh is made with PLANE82 elements with 8 nodes, the element has nonlinear behavior and can be used for our analysis. The tensile curve is introduced point by point to take into account the non-linearity. The resolution is performed by the Newton-Raphson algorithm and by using the increments of σn/5 in each step for load application. The number of iterations is limited to 1000 cycles to avoid any problems due to the non-convergence.

Three levels of loads are applied to illustrate the effect of the elasto-plastic behavior on the stress concentration. The variation of fatigue results parameters and the variation of fatigue reduction factor (Kf) are also analyzed.

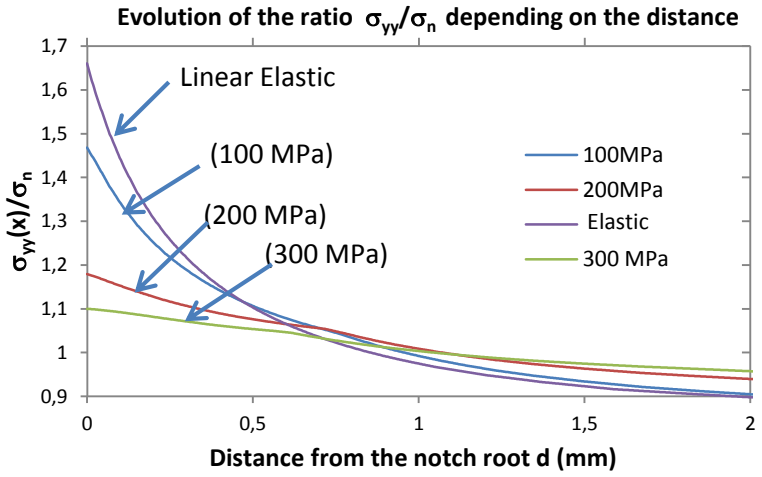

Figure 8 : Load ratio as a function of the distance from the notch root

The presence of the plasticity zone reduces the (Kf) factor which is a function of loading and material behavior. Increasing the load reduce significantly this factor which becomes close to 1, this shows that the life obtained by a linear elastic theory is a more conservative approach. Calculating the stress concentration factor by the model proposed by Glinka Nui and [16] with an opening notch angle of 155 °, give a stress concentration factor Kt = 1.969.

Estimating the effect of the notch on the fatigue strength of the weld
Evaluation the (Kf) factor is performed using the Neuber and Peterson approaches that are more adapted to the elastic range. In the presence of plasticity, the volumetric method is used to derive the (Kf) factor.

Fatigue reduction factor according to Neuber [17] and Peterson's [15] model

Neuber: $$Kf = 1 + \frac{Kt - 1}{1 + \sqrt{\frac{a_n}{\rho}}} \quad (12)$$

With $$a_n = 10^{-\frac{Rm-134}{586}} = 0{,}315 \quad (13)$$

Peterson: $$Kf = 1 + \frac{Kt - 1}{1 + \frac{a_p}{\rho}} \quad (14)$$

With $$a_p = \left(270 \times Rm^{-1}\right)^{1{,}8} = 0{,}432 \quad (15)$$

Kt: Stress concentration factor
ρ: Notch radius
a_n: Neuber factor [24]
a_p: Peterson factor [18]

Fatigue reduction factor according to volumetric approach [1]

$$Kf = \frac{\sigma_{eff}}{\sigma_n} = \frac{1}{X_{eff}\,\sigma_n} \int_0^{X_{eff}} \sigma_{yy}(x) \times (1 + x\chi(x))dx \quad (16)$$

σ_n: Applied load
σ_{eff} : Effective stress calculated by integrating the stress on the effective distance (X_{eff})
$\sigma_{yy}(x)$: Opening stress as a function of the distance from the notch root (x).
$\chi(x)$: Relative stress gradient
X_{eff} : Extent of the effective area located between the notch root and the point where (χ (x)) is minimal.

The evolution of the stress $\sigma_{yy}(x)$ is represented along the (D1) line (figure 7-b) from the point where the stress intensity is high (Figure-7). For a load level of 300 MPa, the inflection point observed on the stress curve allows locating graphically the effective distance, this point is located at a distance of (0.519 mm). The calculation of the mean stress at the effective area gives a value of 315.9 MPa.

The following table shows the values of fatigue reduction factor (Kf) calculated by the three methods and three load levels.

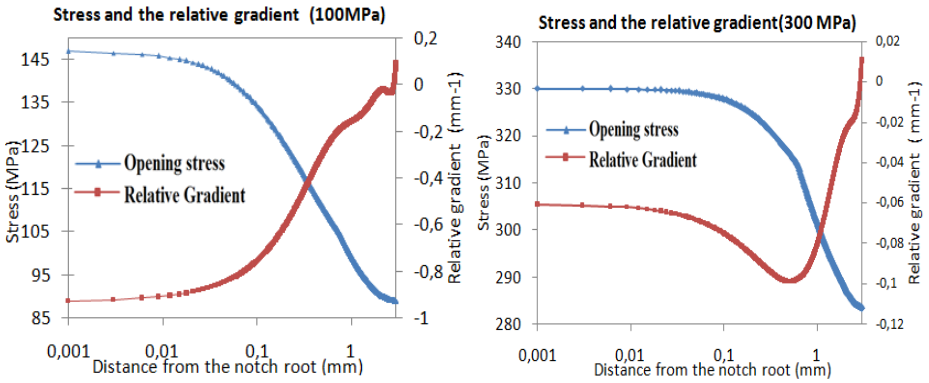

(a) (b)

Figure 9 : Opening stress and relative gradient under different load stress
(a) : 100MPa; (b) : 300 MPa

	σn = 100 MPa			σn = 200 MPa			σn = 300 MPa		
	Neuber	Peterson	Volumetric	Neuber	Peterson	Volumetric	Neuber	Peterson	Volumetric
Kf	1,316	1,341	-	1,114	1,126	-	1,067	1,074	1,053
Kt	1,46			1,17			1,1		

Table 8: Fatigue reduction factor for the butt welded joint

The results show that the fatigue reduction factor (Kf) have a downward trend by increasing the applied load, which will influence the difference between the reference fatigue curve and the fatigue curve with notch effect.

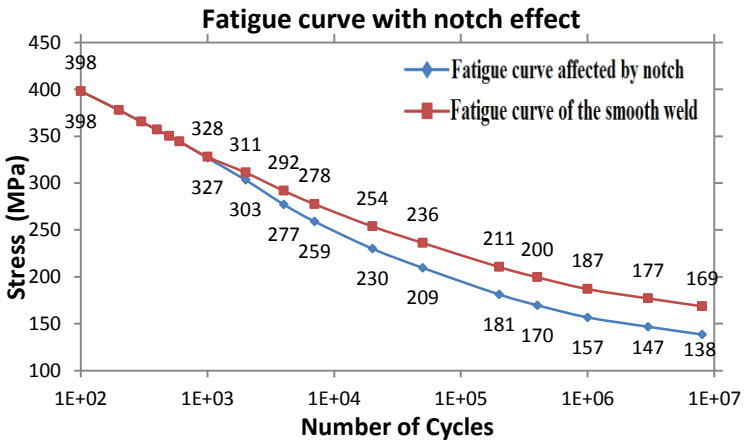

Figure 10 : Reference fatigue curve and the fatigue curve with notch effect

In order to evaluate these values, the results were compared with the fatigue curves prescribed by the British standard BS 7608 [23], the comparison is made with the fatigue curve of class (B) related to smooth butt welded joints and class (D) related to welded joints with root radius loaded transversely. The following table summarizes the calculation parameters according to the BS7608 for a weld root with opening angle of 155°.

Classe (B)				Classe (D)			
C	M	$\sigma(N=10^6)$	$\sigma(N=10^7)$	C	m	$\sigma(N=10^6)$	$\sigma(N=10^7)$
$1{,}01.10^{15}$	4	178,27	74	$3{,}99.10^{12}$	3	158,60	100

Table 9 : Fatigue parameters according to the BS7608

Comparing the results obtained in the table above with the results of the fatigue curve already obtained show a satisfying approximation especially for N = 10^6 cycles. This reconciliation is less for higher life duration; this difference can be justified by a conservative behavior of the standard which is needed to fit with the different steel grades.

3-2 T welded joint

The geometrical parameters and the linear modeling results

The T-joint is known by a high stress concentration factor. The stress field analysis for this type of joint shows that the first micro crack under a tensile load will initiate in the vertical plate (Figure-11). The connecting radius between the weld bead to the central plate is considered to be of 1mm. All geometrical and loading parameters are shown in the following figures.

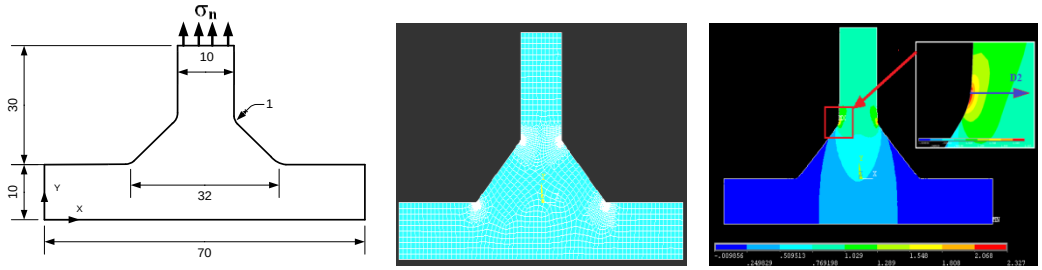

(a) (b) (c)

Figure 11 : T welded joint
(a) : Geometrical and loading parameters;
(b) : Meshed geometry ; (c) : Stress field σyy(x,y) and the analysis direction (D2)

The Load will be applied on the vertical plate. The boundary conditions will be applied on the base plate which will be immobilized by fixing the base surface (x=0) in the vertical direction (Uy = 0), and by fixing its side surface (y=0) in the horizontal direction (Ux = 0).

Elasto-plastic analysis results

The resolution of the elasto-plastic problem will be achieved by using nonlinear finite elements technique. To solve the iterative problem, we will keep the same parameters already used for butt welded joint. The following figure shows the evolution of the ratio between the local stress obtained by elasto-plastic calculation (σyy(x)) and the applied load (σn). The analysis of the evolution of the ratio ($\sigma_{yy}(x)/\sigma_n$) is performed along direction D2 (Figure 11-c), three load levels will be applied during this analysis.

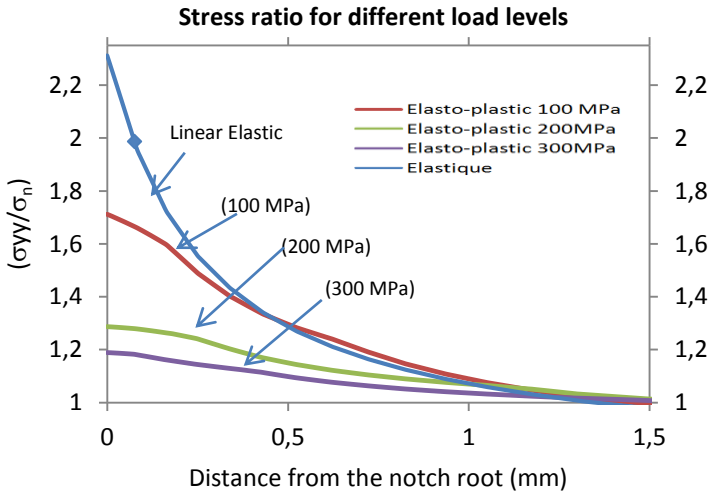

Figure 12 : Evolution curve of the stress ratio ($\sigma_{yy}(x)/\sigma_n$)

Figure-12 shows the significant effect of the plasticity on the (Kf) factor and consequently on the reduction of the fatigue life. This factor which reflects the influence of the notch, becomes less important with increasing applied load, this prove that the reduction in fatigue strength will be smaller in low cycle fatigue.

Notch effect on the fatigue strength

Similarly to the previous case, we will use the evolution of the notch opening stress $\sigma_{yy}(x)$ and its relative gradient to calculate the fatigue parameters by the volumetric method.

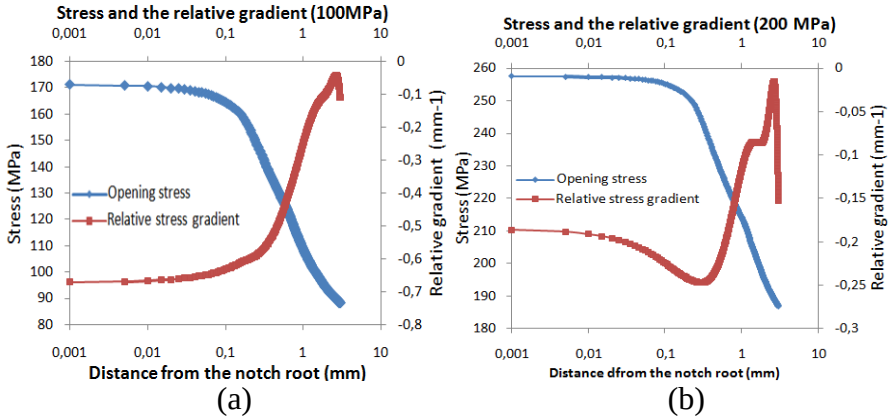

Figure 13: Evolution of the notch opening stress and its relative gradient
(a) : 100 MPa; (b) : 200MPa

Calculating the relative gradient is performed using the regression of the stress curve by a 6 th order polynomial which ensures a correlation factor of 0.998. The results of numerical analysis of the stress field gave the following values of the (Kf) factor.

	σn = 100 MPa			σn = 200 MPa			σn = 300 MPa		
	Neuber	Peterson	Volumetric	Neuber	Peterson	Volumeric	Neuber	Peterson	Volumetric
Kf	1,456	1,496	-	1,242	1,263	1,229	1,121	1,132	1,149
Kt	1,711			1,377			1,188		

Table 10 : Fatigue reduction factor (Kf) for T weld joint

The evolution of the (Kf) factor is approximated by linear regression using the four values obtained in the various loads applied.

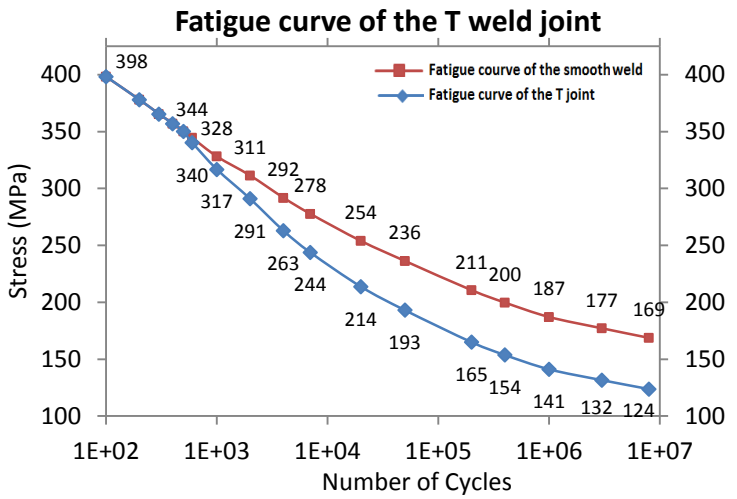

Figure 14 : Fatigue curve of the T joint compared to the curve of the smooth weld

The difference between the reference fatigue curve (smooth weld) and the fatigue curve of the T joint is more important near the endurance limit. The difference reached significant values of 45 MPa. For T welded joints, the values prescribed by the IIW international standard [7] is limited between 80 MPa and 70 MPa for a life duration of ($N = 2.10^6$), the BS 7608 standard recommends a value of 85 MPa given for a minimum misalignment [23]. An analysis of the experimental results given by [11] shows an endurance limit of 110 MPa. The variability of the results obtained for the T-joints comes from the significant effect of the thickness of the central plate on the endurance limit. The experimental work achieved by Gurney [5] illustrate the effect of the geometrical parameters of the welded joints, these results showed a drop in the fatigue limit from 130 MPa to 90 MPa by increasing the thickness from 10 to 100mm.

The thickness effect influence considerably the endurance of the T-joints, the values recommended by the two standards mainly deal with the resistance of thick structures which justifies the endurance limit imposed. The conservative nature of these standards is also required to ensure maximum reliability of structures under the various conditions of service. The aspect of these standards tends to prescribe an endurance limit (σ_D) for a family of steels without distinction, which leads to recommend the lowest resistance that may be encountered.

4- Conclusion

The method used in this work provides a means to calculate the fatigue strength of welded joints based mainly on experimental data obtained from static mechanical tests (tensile tests and hardness). The characterization results of weld bead provide a knowledge base that will shed light on the fatigue behavior by using the remarkable correlation between the static mechanical properties and fatigue properties. Adopting the approach based on the local deformation (ε-N) allows us to take into account the effect of the elastic and plastic deformation components which can cover a large area of the fatigue life and will allow to draw the curve (σ-N) with more precision.

The calculation of the Wohler curve with this approach gave us very comparable values to fatigue results obtained on materials that have a closer behavior to our steel. These results show that this method can be applied in situations where characterization by fatigue tests represents financial constraints or other constraints related to the duration needed to obtain results.

The fatigue curve obtained for the butt welded joint offer an acceptable accuracy. The analysis of the obtained curve shows a significant effect of welding notches on the reduction of the fatigue life duration more particularly in the vicinity of the endurance limit. In the case of T-joints, the gap between the obtained results and standardization data is more remarkable. This difference in fatigue strength is due to the effect of thickness. The endurance limits recommended by the standardizations consider welded joints with significant thicknesses which reduces the endurance limit.

References

[1] H. Adib, G. Pluvinage, Theoretical and numerical aspects of the volumetric approach for fatigue life prediction in notched components, *International Journal of Fatigue*, **25** (2003), 67-76. http://dx.doi.org/10.1016/s0142-1123(02)00040-3

[2] C. Boller, T. Seeger, *Materials Data for Cyclic Loading*, Elsevier, 1987

[3] J. E. Brumbaugh, R. Miller, Welding Pocket Reference, Appendix A, Wiley, 2007, 397-398.

[4] N. E. Dowling, Mechanical Behavior of Materials, Pearson Education, (2013), 163-164.

[5] T. R. Gurney, *The Fatigue Strength of Transverse Fillet Welded Joints, A Study of the Influence of Joint Geometry*, Abington Publishing, 1991.

[6] Y. Higashida, J. D. Burk, F. V. Lawrence, Strain-Controlled Fatigue Behavior of ASTM A36 and A514 Grade F Steels and 5083-0 Aluminum Weld Materials, *Welding Research Supplement* (AWS), (1978), 344-334.

[7] A. Hobbacher, *Fatigue design of Welded joints and components - Recommendations of IIW*, Abington Publishing, 1996.

[8] S. Kou, *Welding Metallurgy*, John Wiley and Sons, 2003. http://dx.doi.org/10.1002/0471434027

[9] C. Laird, Fatigue, *Material Science and Engineering*, (1976), 187-191. http://dx.doi.org/10.1016/0025-5416(76)90069-0

[10] Y. L. Lee, M. E. Barkey, Hong-Tae Kang, *Metal Fatigue Analysis Handbook*, Elsevier, 2012.

[11] Lloyd's Register of shipping, *Influence of Goemtery on the Fatigue Strength of T-butt Joints*, Offshore technology report, 1995.

[12] Z. Lopez, A. Fatemi, A method of predicting cyclic stress-strain curve from tensile properties for steels, *International Journal of Fatigue*, **556** (2012), 540-550. http://dx.doi.org/10.1016/j.msea.2012.07.024

[13] P. P.Milella, *Fatigue and Corrosion in Metals*, Springer, 2013. http://dx.doi.org/10.1007/978-88-470-2336-9

[14] H. F. Moore, J. B. Kommers, *The Fatigue of Metals*, McGRAW-HILL, 1927.

[15] R. E. Peterson, Notch-sensitivity, Westinghouse Research Laboratories, (1959), 293-306.

[16] G. Pluvinage, Fracture and fatigue emanating from stress concentrators, *Springer Netherlands*, 2003. http://dx.doi.org/10.1007/1-4020-2612-9

[17] D. Radaj, P. Lazzarin, F. Berto, Generalized Neuber concept of fictitious notch rounding, *International Journal of Fatigue*, **51** (2013), 105-115. http://dx.doi.org/10.1016/j.ijfatigue.2013.01.005

[18] D. Radaj, C. M. Sonsino and W. Fricke, *Fatigue Assessment of Welded Joints by Local Approaches*, CRC Press, 2006.

[19] W. Ramberg, W. R. Osgood, Description of stress-strain curves by Three parameters, National Advisory Committee for Aeronautics, Technical note no. 902, (1943), 1-14.

[20] M. L. Roessle, A. Fatemi, Strain-controlled fatigue properties of steels and some simple approximations, *International Journal of Fatigue*, **22** (2000), 495-511. http://dx.doi.org/10.1016/s0142-1123(00)00026-8

[21] R. Sowerby, D. K. Uko, Y. Tomita, A Review of Certain Aspects of the Bauschinger Effect in Metals, *Materials Science and Engineering*, **41** (1979), 43-58. http://dx.doi.org/10.1016/0025-5416(79)90043-0

[22] Steel Market Development Institute's, Bar Steel Fatigue Database. http://barsteelfatigue.autosteel.org.

[23] R. I. Stephens, A. Fatemi, R. R. Stephens, H. O. Fuchs, *Metal Fatigue*, Wiley Interscience, 2000.

[24] L. Susmel, *Multiaxial Notch Fatigue*, CRC Press, 2009. http://dx.doi.org/10.1533/9781845695835

Received: March 25, 2016; Published: May 19, 2016